Title: Tumor-associated changes in intestinal epithelial cells cause local accumulation of KLRG1$^+$ GATA3$^+$ regulatory T cells in mice

Short title: Intestinal epithelial cells control effector Treg accumulation

Authors: Holger Meinicke [1,2,3,8], Anna Bremser [1,2,8], Maria Brack[1,2,6], Paulina Akeus [4], Claire Pearson[5], Samuel Bullers[5], Katrin Hoffmeyer [1], Marc P. Stemmler [1,7], Marianne Quiding-Järbrink [4], Ana Izcue [1,2]

Affiliations: [1] Max Planck Institute of Immunobiology and Epigenetics, Stübeweg 51, D-79108 Freiburg, Germany.

[2] Center for Chronic Immunodeficiency (CCI), University Medical Center Freiburg and University of Freiburg, Breisacher Straße 117,D-79106 Freiburg, Germany.

[3] Department of Pediatrics and Adolescent Medicine, University Medical Center, Mathildenstrasse 1, 79106 Freiburg, Germany.

[4] Dept of Microbiology and Immunology, Institute of Biomedicine, the Sahlgrenska Academy at the University of Gothenburg, 405 30 Göteborg, Sweden

[5] The Kennedy Institute of Rheumatology, University of Oxford, Roosevelt Drive, Headington, Oxford OX3 7FY, UK

[6]Current address: Roche AG, Wagistrasse 18, 8952 Schlieren, Switzerland

[7]Current address: Department of Experimental Medicine I, Nikolaus-Fiebiger Center for Molecular Medicine, University of Erlangen-Nuremberg, Glueckstr. 6, 91054 Erlangen, Germany

Corresponding author: Ana Izcue, Max Planck Institute of Immunobiology and Epigenetics, Stübeweg 51, D-79108 Freiburg, Germany.

Additional Title Page Footnotes: [7]H.M. and A.B. contributed equally to this work.

Abbreviation list:
Treg: CD4$^+$ Foxp3$^+$ regulatory T cells
EMT: epithelial to mesenchymal transition
CRC: colorectal cancer

Key Words: Regulatory T cells, mucosa, tumor immunology, cell surface molecules

Summary

$CD4^+$ $Foxp3^+$ regulatory T cells (Treg) include differentiated populations of effector Treg characterized by the expression of specific transcription factors. Tumors, including intestinal malignancies, often present with local accumulation of Treg that can prevent tumor clearance, but how tumor progression leads to Treg accumulation is incompletely understood. Here using genetically modified mouse models we show that ablation of E-cadherin, a process associated with epithelial to mesenchymal transition (EMT) and tumor progression, promotes the accumulation of intestinal Treg by the specific accumulation of the $KLRG1^+$ $GATA3^+$ Treg subset. Epithelial E-cadherin ablation activates the β-catenin pathway, and we find that increasing β-catenin signals in intestinal epithelial cells also boosts Treg frequencies through local accumulation of $KLRG1^+$ $GATA3^+$ Treg. Both E-cadherin ablation and increased β-catenin signals resulted in epithelial cells with higher levels of IL-33, a cytokine that preferentially expands $KLRG1^+$ $GATA3^+$ Treg. Tumors often present reduced E-cadherin expression and increased β-catenin signaling and IL-33 production. Accordingly, Treg accumulation in intestinal tumors from $APC^{min/+}$ mice was exclusively due to the increase in $KLRG1^+$ $GATA3^+$ Treg. Our data identify a novel axis through which epithelial cells control local Treg cell subsets, which may be activated during intestinal tumorigenesis.

Introduction

Foxp3-expressing regulatory T cells (Treg) are essential for immune homeostasis, especially in the gut. However, Treg can also contribute to pathogenesis, most notably by inhibiting protective immune responses to tumors in mice and humans (1). Therefore Treg must be kept under strict control. Intestinal epithelial cells play an active role in immune homeostasis by keeping at bay the intestinal microbiota, and they also participate in the modulation of the immune system (2-5). However, whether changes in epithelial cells affect gut Tregs is still unknown.

Treg differentiate into diverse effector subsets that can have organ-specific properties (6, 7). Several effector Treg subsets have been described in the mouse gut, including Helios$^-$ RORγt$^+$ Treg, which develop in response to microbial factors, and the GATA3$^+$ Treg subset that arises independently of the microbiota (reviewed in (8)). In addition to the expression of distinctive transcription factors, Treg subpopulations can express surface receptors such as KLRG1, which can be found on a significant proportion of gut Treg and is considered a marker of terminally differentiated Treg (9, 10). In humans, accumulation of effector Treg but not of other FOXP3$^+$ populations are associated with a worse prognosis in colorectal cancer (CRC) (11), and two recent studies have confirmed that human tumor-infiltrating Treg have a specific distinct phenotype (12, 13).

Here we use mouse models to examine whether tumor-related alterations of epithelial cells can per se affect intestinal Treg populations. We have focused on E-cadherin, a key epithelial cell adhesion molecule that also affects intracellular signaling. We used a mouse model of cell-specific cadherin switch in which E-cadherin is replaced by its homologue N-cadherin in the intestinal epithelium (14), mimicking the

cadherin switch that takes place during epithelial to mesenchymal transition (EMT), a key step in tumor progression. We found that mice with E-cadherin-deficient epithelium present with a striking expansion of effector-like KLRG1^{+} GATA3^{+} Foxp3^{+} cells. Using additional genetically modified mouse models, we linked KLRG1^{+} GATA3^{+} Treg accumulation to increased epithelial β-catenin signals, which promote intestinal IL-33 expression. Spontaneous intestinal tumors from mice with increased β-catenin signals also presented strong specific accumulation of KLRG1^{+} GATA3^{+} Treg. Our data highlight an unappreciated role for intestinal epithelial cells in controlling the size of the gut Treg compartment. Given the role of regulatory T cells in maintaining an immunosuppressive environment in tumors, the axis linking epithelial β-catenin to KLRG1^{+} GATA3^{+} Treg accumulation could be an interesting therapeutic target.

Materials and Methods

Mouse strains

Wild-type C57BL/6, C57BL/6 Cdh1$^{Ncad/fl}$ Villin Cre^{+} (14), congenic B6.SJL-*Cd45*, BALB/c *Il10*$^{-/-}$, C57BL/6 *Rag2*$^{-/-}$ and Ctnnb1$^{(Ex3)fl/+}$ Lgr5-EGFP-IRES-ERT2:Cre^{+}(15, 16) mice were kept and bred under SPF or GF conditions at the animal facility of the Max-Planck Institute of Immunobiology and Epigenetics. For tamoxifen treatment, Ctnnb1$^{(Ex3)fl/+}$ Lgr5-EGFP-IRES-ERT2:Cre^{+}mice and controls were injected intraperitoneally every other day with 200µg tamoxifen per day in sunflower oil for a total of three doses, and analyzed 22 days after the last injection. All experiments were approved by the institutional review board of the Max Planck Institute of Immunbiology and Epigenetics and the local government in Freiburg. APC$^{min/+}$ mice on a C57BL/6 background were kept and bred under SPF conditions in filter-top cages at the University of Gothenburg and analyzed between 18-21 weeks of age. The study was approved by the animal ethics committee at the University of Gothenburg.

Isolation of leukocytes from the lamina propria and epithelial cells

Leucocytes from the lamina propria were isolated as described (17, 18). Briefly, small intestine and colon were removed and cleaned. Samples (around 5 mm long) were removed for histology, and the rest of the colon was used for lymphocyte isolation. For young Cdh1$^{\Delta IEC}$ mice and littermate controls, the whole small intestine was used for lymphocyte isolation after removal of samples for histology. For IL-10-deficient and DSS-treated mice and controls, the distal small intestine was used for lymphocyte isolation. The proximal and distal parts of Ctnnb1$^{(Ex3)fl/+}$ Lgr5-EGFP-

IRES-ERT2:Cre^{+}mice and controls were used for isolation as indicated. For APC$^{min/+}$ and control mice, the entire small intestine was used for isolation. After washing with ice-cold PBS, intestines were washed twice in Hank's Balanced Salt Solution (HBSS) containing 5 mM EDTA and 10 mM HEPES at 37°C to remove the epithelial cell layer. The tissue was then minced finely and digested 3 times in HBSS containing Dispase (5 units/ml; BD Biosciences), Collagenase IV (0.5 mg/ml; Worthington, Lakewood, NJ) and DNaseA (0.5 mg/ml; AppliChem, Darmstadt, Germany), at 37°C with constant shaking. Supernatants were collected and lymphocytes were enriched after a gradient centrifugation using buffered Percoll (GE Healthcare, Freiburg, Germany).

DSS-colitis

Induction of colitis through dextran sulfate-sodium (DSS) was done as previously described (19). Briefly, animals were given 3% DSS (MP Biomedicals, Santa Ana, CA) in the drinking water during 8 days. Weight loss was monitored as a sign of disease progression. Mice were sacrificed at day 8 for analysis and the establishment of colitis was checked by macroscopical signs (swollen, pale colon).

Antibodies and Flow cytometry

Single cell suspensions were stained in 96-well plates (10^6 cells per well). The following conjugated antibodies were purchased from eBioscience: TCR-β (H57-597), CD3 (145-2C11), CD4 (GK 1.5), KLRG1 (2F1), CD103 (2E7), CD44 (IM7), CD45RB (C363.16A), CD62L (MEL-14), CD69 (H1.2F3), CD45.1 (A20), CD45.2 (104), CD25 (PC61.5), Foxp3 (FJK-16s), GATA3 (TWAJ), Tbet (3C8), Rorγ (B2D), Helios (22F6), IRF4 (3E4), Ki67 (20Raj1), Nur77 (12.14) and CTLA4 (UC10-4B9). Anti-IL-33Rα

antibody (DIH9) was purchased from Biolegend. Intracellular staining was performed with the eBioscience permeabilization and fixation kit. Anti-Bcl-2 (3F11) was purchased from BD Biosciences. Dead cells were excluded by staining with Fixable Viability Dye (eBioscience). For cytokine staining, cells were incubated for 4 hours at 37°C in the presence of PMA, ionophore and Brefeldin A as described (18), and stained with antibodies against IL-2 (JES6-5H4), IL-5 (TRFK5), IL-13 (13A), IL-17 (17B7) or IFN-γ (2E2). All flow cytometry experiments were acquired using a BD LSR II cytometer or LSR Fortessa (BD). Flow Jo Version 8.8.7 was used for data analysis. For calculating total cell numbers, cell concentrations were counted with a CASY cell counter (Roche) and the total numbers multiplied by the frequency of $CD4^+$ $Foxp3^+$ cells among living cells.

Treg culture

Flat bottom 96 well plates were pre-coated with 5 µg/purified anti- mouse CD3ε (145-2C11, Biolegend) at 37°C for a minimum of 30 minutes. FACS-sorted $CD4^+CD25^+$ cells from wild-type C57BL/6 were seeded at 10^5 cells/ well and cultured in RPMI containing 10% fetal calf serum and 1U/ml IL-2 or 5 ng/ml/ IL-33 where indicated (PeproTech, Hamburg, Germany). After 8h or 3 days of incubation at 37°C, cells were harvested and analysed by flow cytometry. To test in vitro suppression, 10^5 $CD4^+$ $CD25^-$ T cells were cultured with 10^5, 5 10^4 or 10^4 $CD4^+$ $CD25^+$ $KLRG1^-$ or $CD4^+$ $CD25^+$ $KLRG1^-$ cells in the absence of exogenous IL-2.

Quantitative real-time PCR

Intestinal epithelial cells were isolated after 37ºC incubation with RPMI/5%FCS/2.5mM EDTA. Total RNA was extracted with TRI reagent (SIGMA)

and was reverse-transcribed with QuantiTect Reverse Transcription Kit (Qiagen) following the instructions of the manufacturer. Amplification was performed using Absolute Blue qPCR SYBR low ROX mix (Thermo Scientific). Values were normalized to *Hprt*. Primer sequences were taken from (20) (*Il33*) and (21)(*Hprt*).

Statistical analysis

Statistical analysis was performed using GraphPad Prism using a 2-tailed unpaired Student's t test when only two groups were tested, or ANOVA with Bonferroni-Post-test where more than two groups were tested. Differences were considered statistically significant when $p < 0.05$. Bars represent arithmetical mean except for bars in graphs with a logarithmic y axis, which represent median.

For the analysis of genes altered in the intestinal cadherin switch model, GSE81920 was analyzed using the Multiplot module from GenePattern (22). Genes with cytokine activity were identified with AmiGO Gene Ontology term GO:0005125, *Mus musculus* (23).

Results

Ablation of E-cadherin on intestinal epithelial cells induces KLRG1$^+$ Treg accumulation in the gut

We used a model of gut-specific cadherin replacement that mimics the cadherin switch observed during EMT in oncogenic progression (14). In our model, one E-cadherin allele is replaced by N-cadherin while the other allele is floxed and conditionally deleted in intestinal epithelial cells after expression of an intestinal epithelial cell-restricted Villin-Cre transgene (Cdh1$^{fl/NcadKI}$ VilCre$^+$, denoted Cdh1$^{\Delta IEC}$

mice). In the absence of Cre expression, N-cadherin is co-expressed together with E-cadherin in all E-cadherin expressing organs; this ectopic N-cadherin expression does not detectably affect the mouse phenotype (14). In VilCre^{+} mice where E-cadherin is deleted in intestinal epithelial cells, N-cadherin preserves cell adhesion and the intercellular junctions in the gut epithelium (14), although the mice develop intestinal inflammation (manuscript in preparation). Nevertheless, we observed that the frequencies of Th1 (IFN-g^{+}), Th2 (IL-5^{+}) and Th17 (IL-17A^{+}) effector CD4^{+} T cells were not increased in the gut from Cdh1$^{\Delta IEC}$ mice compared to control littermates (Fig 1A). The frequency of IL-2^{+} CD4^{+} T cells was also not increased in the gut from Cdh1$^{\Delta IEC}$ mice; actually, the frequency of IL-2-expressing CD4^{+} T cells was reduced compared to controls in the gut, but not in lymphoid organs (Fig 1A and Fig S1). In contrast, when we examined the Foxp3^{+} T cell (Treg) compartment in Cdh1$^{\Delta IEC}$ mice, we found a striking increase in the frequency of Treg in the small intestine and colon, with a smaller accumulation in spleen and MLN (Fig 1B). Neither the co-expression of E-cadherin and N-cadherin (Cdh1$^{fl/Ncad}$ mice) nor mono-allelic E-cadherin deletion (Cdh1$^{fl/+}$ VilCre^{+} mice) affected the frequency of Foxp3^{+} cells (Fig S1A). Cdh1$^{\Delta IEC}$ mice are runty and about half the size of their littermates (14). Their smaller spleen size, which corresponds with their smaller body size (manuscript in preparation), likely explains the lower cell numbers and total Treg cell numbers observed in the spleen from Cdh1$^{\Delta IEC}$ mice (Fig 1B). In contrast, despite their smaller body size, absolute Treg numbers were increased in the MLN and gut from Cdh1$^{\Delta IEC}$ mice compared to littermates (Fig 1B).

We then determined the expression of the CD103 and KLRG1 on the accumulating Treg. Both CD103 and KLRG1 have been proposed as markers of

activated Treg; in addition, both receptors can recognize E-cadherin. KLRG1$^+$ cells, irrespective of CD103 co-expression, were drastically increased among colonic Foxp3$^+$ cells in Cdh1$^{\Delta IEC}$ mice (Fig 1C and S1B), while there was a trend towards reduction of CD103$^+$ KLRG1$^-$ cells and the frequency of total CD103 cells was unchanged. In fact, the increase in Treg frequency among CD4$^+$ T cells was mainly the result of increased KLRG1$^+$ Treg frequency in all organs, and the frequency of KLRG1$^-$ Treg was in contrast unaffected (Fig 1D, E). This suggests that epithelial E-cadherin typically restrains accumulation of KLRG1$^+$ Treg in the gut, and that epithelial loss of E-cadherin leads to local accumulation of KLRG1$^+$ Treg.

Although Treg accumulation was strongest in the gut, the frequency of KLRG1$^+$ Foxp3$^+$ Treg was elevated in all organs observed, pointing to a general increase in Treg rather than altered migration of Treg to the intestine. Interestingly, the elevated KLRG1$^+$ frequency was specific for Foxp3$^+$ T cells, as the frequency of KLRG1$^+$ cells in other T cell populations was not changed (Fig S1C). KLRG1$^+$ Treg have been shown to accumulate in some models of inflammation (24, 25). However, there was no specific accumulation of KLRG1$^+$ Treg in two classical models of colitis that we tested, microbiota-independent acute DSS-induced inflammation and the microbiota-dependent, chronic colitis that develops in IL-10-deficient mice (Fig. 2). This indicates that intestinal inflammation does not necessarily result in increased levels of KLRG1$^+$ Treg.

Accumulating KLRG1$^+$ Foxp3$^+$ T cells have a GATA3$^+$ effector Treg phenotype

In humans, three populations of FOXP3-expressing cells have been described: naïve Treg, effector Treg, and $FOXP3^+$ cells without regulatory activity (non-Treg) (26). These populations are associated with differential clinical outcomes in cancer. High levels of $FOXP3^+$ effector Treg in CRC tumors are associated with a poor prognosis, while high levels of $FOXP3^+$ non-Treg cells are associated with a better prognosis (11) underscoring the contribution of functional Tregs to development/maintenance of tumors. Populations of effector Treg and populations of $Foxp3^+$ cells producing inflammatory cytokines have also been described in mice (27, 28).

We therefore sought to characterize the accumulating $KLRG1^+$ Treg cells in $Cdh1^{\Delta IEC}$ mice. $KLRG1^+$ $Foxp3^+$ T cells have been described to be terminally differentiated effector Treg with suppressive activity *in vivo* and *in vitro* ((9, 24, 25) and Fig S2A). To determine whether the $KLRG1^+$ Treg population in $Cdh1^{\Delta IEC}$ mice is phenotypically equivalent to the described populations of $KLRG1^+$ Treg, or whether it results from KLRG1 induction on different Treg subpopulations, we performed a phenotypic analysis of $KLRG1^+$ Treg cells isolated from the MLN of $Cdh1^{\Delta IEC}$ and control littermates. As previously described (24), $KLRG1^+$ Treg exhibited a phenotype consistent with activated/effector Treg, characterized by expression of CTLA-4, IRF4 and Helios, low levels of Bcl-2, high levels of CD44 and low levels of CD62L (Fig 3A-B, Fig S2B-E). $KLRG1^+$ Treg were enriched for proliferative $Ki67^+$ cells at a similar extent in $Cdh1^{\Delta IEC}$ and control mice, suggesting that E-cadherin does not affect $KLRG1^+$ Treg proliferation in this model (Fig 3C). While $KLRG1^+$ and $KLRG1^-$ Treg populations clearly phenotypically differed from each other, cadherin switch did not affect the phenotype of the $KLRG1^+$ Treg subpopulation, suggesting that the absence of

E-cadherin does not induce KLRG1 across all Treg subsets, but instead increases the accumulation of the KLRG1$^+$ effector Treg subset.

Effector Treg have been further divided into subpopulations expressing transcription factors mirroring the other CD4$^+$ T helper subsets, such as T-bet, GATA3 and RORγt (6, 8). The expression of the transcription factor GATA3 in intestinal Treg was mostly restricted to KLRG1$^+$ cells in Cdh1$^{\Delta IEC}$ and control mice (Fig 3D-E), while we did not find a correlation of the transcription factors T-bet and RORγt with KLRG1 expression in Treg (Fig 3D-E), suggesting that GATA3 expression is mainly limited to KLRG1$^+$ Treg.

GATA3 expression is essential for the anti-inflammatory activity of the GATA3$^+$ subset of Treg (29-31), but high levels of GATA3 can turn a Treg into a *bona fide* Th2 pro-inflammatory T cell (32). Interestingly, the expression of GATA3 by Treg in Cdh1$^{\Delta IEC}$ mice was lower than in the small GATA3$^+$ fraction among Foxp3$^-$ T cells (Fig 3E), fitting with Treg-like rather than Th2-like GATA3 expression. Similar to genuine Treg, KLRG1$^+$ Treg expressed high levels of Foxp3 (Fig 3E), and did not produce any of the pro-inflammatory cytokines we tested (Fig 3F, Fig S2F). Hence, they do not correspond to the human proinflammatory FOXP3$^+$ fraction but to a *bona fide* effector subset.

In summary, the KLRG1$^+$ Treg population accumulating in the gut of Cdh1$^{\Delta IEC}$ mice is phenotypically similar to the one in control Cdh1$^{fl/Ncad}$ and wild-type mice. KLRG1$^+$ Foxp3$^+$ cells display an activated GATA3$^+$ Treg phenotype with high levels of Foxp3 like *bona fide* Treg, suggesting that epithelial-specific cadherin switching induces the local accumulation of a subset of effector Treg rather than naïve Treg or inflammatory Treg.

Increased β-catenin signals induce the accumulation of KLRG1$^+$ Treg in the gut

Cdh1$^{\Delta IEC}$ mice show alterations in the epithelial β-catenin pathway, with β-catenin target genes already increased in epithelial cells from newborn Cdh1$^{\Delta IEC}$ mice (14). We set out to determine if alterations in β-catenin also increase the frequency of intestinal Treg. β-catenin binds to cadherins at the cell membrane, but detached β-catenin can translocate into the nucleus and activate Wnt target genes (reviewed in 33). The activation of the Wnt/β-catenin pathway is a hallmark of intestinal tumors. In order to determine if the increased levels of β-catenin signals observed in epithelial cells after cadherin switch can induce the accumulation of intestinal Treg, we used a model of tamoxifen-induced recombination in intestinal stem cells that deletes the β-catenin exon required for tagging the protein for degradation (15, 16). Upon recombination, a stable form of β-catenin is generated that can signal in the absence of Wnt ligands, and the progeny of the recombined intestinal stem cells therefore exhibits constitutive β-catenin signaling.

We analyzed the mice three weeks after the tamoxifen injection, when active β -catenin accumulates in the nucleus. We found that enhanced β-catenin signals increased Treg accumulation in the small intestine of adult mice (Fig 4A), and also increased the accumulation of KLRG1$^+$ Treg (Fig 4B). Indeed, the increased Treg frequency was due to an augmentation in KLRG1$^+$ Foxp3$^+$ T cells, while no differences were seen in the proportions of KRLG1$^-$Foxp3$^+$ cells (Fig 4C, D), similarly to the pattern observed in mice with epithelial-specific cadherin switch. In keeping with the published regional variations of β-catenin activation (16), KLRG1$^+$ Treg accumulation was more marked in the small intestine compared to the colon. As in Cdh1$^{\Delta IEC}$ mice, the KLRG1$^+$ Treg were

GATA3$^+$ (Fig 4E). Hence, increased β-catenin signaling in intestinal epithelial cells recapitulates the KLRG1$^+$ Foxp3$^+$ Treg accumulation observed in Cdh1$^{\Delta IEC}$ mice.

Intestinal tumors from APC$^{min/+}$ mice accumulate KLRG1$^+$ Treg

β-catenin signals are often increased in tumor cells of epithelial origin, including intestinal tumors (34). On the other hand, Treg accumulate in many types of tumors, where they can suppress the cytotoxic antitumoral response (6, 35). To assess whether KLRG1$^+$ Treg are also specifically increased in a model of spontaneous gut tumor development with enhanced β-catenin signaling, we analyzed the Treg populations in intestinal tumors from APC$^{min/+}$ mice (36). These mice have a heterozygous mutation in *Apc*, a gene encoding an essential protein to target β-catenin for proteosomal degradation that is mutated in around 80% - 90% of human CRC tumors (37). Upon spontaneous mutations in the second *Apc* allele, β-catenin is stabilized and aging APC$^{min/+}$ mice therefore spontaneously develop intestinal tumors, primarily in the small intestine (reviewed in 38). It has been previously shown that Treg accumulate in these tumors and impair cytotoxic responses (39). In accordance with published data, we found that most tumors had increased Treg frequencies (Fig 5A). When we analyzed KLRG1 expression in these mice, we found that KLRG1$^+$ GATA3$^+$ Treg were predominant among Treg from the tumors, but not from the surrounding tissue (Fig 5B, C). As in mice with cadherin switch or with an epithelial-specific increase in β-catenin, the increased Treg frequency in intestinal tumors from APC$^{min/+}$ mice was exclusively due to an increase in the KLRG1$^+$ Treg population (Fig 5D,E). In accordance with the other models with increased β-catenin signals, the frequency of KLRG1$^+$ Foxp3$^+$ Treg was increased but the percentage of KLRG1$^-$ Foxp3$^+$ Treg remained unchanged. The

mice without Treg accumulation in tumors ("Treg^{lo} tumors") did not show increased KLRG1$^+$ Treg either. Hence, enhanced β-catenin signaling also drives the specific accumulation of the KLRG1$^+$ GATA3$^+$ Treg subset in spontaneous intestinal tumors.

IL-33 is induced in epithelial cells with increased β-catenin activity and promotes KLRG1$^+$ accumulation

To identify a molecule that could mediate the communication between β-catenin signals in epithelial cells and accumulation of KLRG1$^+$ Treg, we compared the mRNA expression profile of intestinal epithelial cells from young Cdh1$^{\Delta IEC}$ and control mice, focusing on genes with cytokine or chemokine activity. The analysis identified the alarmin *Il33* as a gene specifically increased in epithelial cells lacking E-cadherin (Fig 6A). IL-33 is known to be upregulated in APC^{min} tumors (20), and we found that increased β-catenin signals also promote IL-33 induction in the intestinal epithelium (Fig 6B, C). Hence, IL-33 is induced in epithelial cells with activated β-catenin.

IL-33 promotes the accumulation of GATA3$^+$ Treg in the intestine (40), and KLRG1$^+$ Treg express high levels of the IL-33 receptor upon stimulation (Fig 6D). Accordingly, IL-33 induced the accumulation of KLRG1$^+$ Treg in vitro (Fig 6E). The accumulation was due to the expansion of existing KLRG1$^+$ Treg, as IL-33 did not induce KLRG1 expression on KLRG1$^-$ Treg upon culture (Fig 6F). IL-33 favored KLRG1$^+$ Treg cell division as well as accumulation of undivided cells (Fig 6G), indicating that it can enhance both proliferation and survival of KLRG1$^+$ Treg. Therefore our data indicate that IL-33 can link malignancy-associated epithelial changes to the accumulation of a specific Treg subset in mouse intestine.

Discussion

Treg in the gut are controlled by local factors (8), but the role of epithelial cells in this crosstalk, and how tumoral changes affect intestinal Treg, is less well understood. Our results indicate that changes associated with tumor progression, namely cadherin switching and increased β-catenin activity, cause effector Treg accumulation in the gut.

Beyond their functions in cell-cell adhesion, cadherins also affect intracellular signals. E-cadherin directly binds the Wnt pathway mediator β-catenin, and a previous report showed that β-catenin transcriptional targets are increased in our model of intestinal cadherin switch (14). Using a model of induced epithelial β-catenin signaling (16, 41), we found that increased β-catenin signals in epithelial cells recapitulate the $KLRG1^+$ Treg accumulation found in the cadherin switch model. Hence, the altered epithelial signals resulting from reduced E-cadherin can promote the specific accumulation of KLRG1-expressing Treg. We have identified IL-33 as a likely candidate to mediate $GATA3^+$ $KLRG1^+$ Treg accumulation in response to increased epithelial β-catenin signals. The frequency of IL-2-expressing $CD4^+$ T cells was not increased, but rather decreased, in $Cdh1^{\Delta IEC}$ mice. While IL-2 plays an important role in Treg cell maintenance, it is not the only factor that drives Treg accumulation. The fact that IL-2 is not increased in the gut of $Cdh1^{\Delta IEC}$ mice suggests that other factors drive Treg maintenance in this setting. We find that IL-33 is increased in epithelial cells with ablated E-cadherin expression or increased β-catenin signals, as well as in epithelial cells from APC^{min} tumors (20), and that it directly promotes $KLRG1^+$ Treg survival and proliferation. It will be of interest to assess the levels of IL-33 in different models of

intestinal inflammation, such as Th2-driven models or in the DSS model, and to check its effect on KLRG1$^+$ Treg accumulation in these settings. Whether β-catenin directly induces IL-33, or whether the increase in IL-33 is secondary to changes induced by β-catenin signaling, remains to be investigated.

Cadherin switch, β-catenin signals, and Treg accumulation are all linked to cancer. Treg often accumulate in human and mouse tumors, and they are considered to contribute to the immunosuppressive environment that protects tumors from immune attack (1). Indeed, in human CRC effector Treg accumulation is associated with a worse disease-free outcome (11). Here we show that Treg accumulation in spontaneous tumors in the APC$^{min/+}$ model, which is known to inhibit the accumulation of effector T cells (39), is exclusively due to KLRG1$^+$ GATA3$^+$ Treg. We do not know the exact process leading to the local accumulation of KLRG1$^+$ GATA3$^+$ Treg. KLRG1$^+$ Treg frequencies in Cdh1$^{\Delta IEC}$ mice were increased in all organs analyzed, suggesting that migration is not the mechanism leading to Treg accumulation. Accordingly, IL-33 increased KLRG1$^+$ Treg numbers and frequencies in an in vitro model, where migration is excluded. We found that IL-33 increases both proliferation and survival of existing KLRG1$^+$ cells in vitro. Since KLRG1$^+$ Treg in newborn mice intestine have already a high proliferation rate, as shown in Fig 3C, it is plausible that in the Cdh1$^{\Delta IEC}$ model the major effect of IL-33 is enhancing KLRG1$^+$ Treg survival.

The specific accumulation of a particular effector Treg subset in tumors could have consequences beyond immunosuppression. GATA3$^+$ Treg have been proposed to induce tissue repair through the secretion of amphiregulin (42, 43). Amphiregulin binds the epidermal growth factor receptor (EGFR), which promotes growth of numerous cancers (44), so it is possible that Treg accumulating in tumors promote carcinogenesis

not only through immunosuppression but also by secreting factors supporting cancer cell survival. Along this line, KLRG1$^+$ Treg are enriched for β8 integrin and have an enhanced capacity to activate TGF-β (45), which also favors the oncogenic process. It will be of interest to check whether Treg equivalent to mouse KLRG1$^+$ GATA3$^+$ Treg accumulate in human tumors. Because IL-33 is an alarmin expressed by different tissues (46), the processes described here may play a role in tuning immune regulation in tumours from various organs.

Our results show that increased β-catenin signals promote accumulation of KLRG1$^+$ Treg resulting in a strong increase in Foxp3$^+$ frequencies. Our present findings complement reports on the regulation of tissue repair by KLRG1$^+$ Treg (42, 43), stressing the bidirectional interaction between the immune system and epithelia, and highlight an unappreciated role for intestinal epithelial cells in controlling the size of the gut Treg compartment. This may be important to ensure that protective immunity against invading pathogens is retained. Tumor-associated epithelial changes disrupt this process, which results in the local accumulation of a specific effector Treg subset, underscoring how epithelial cells are important for the maintenance of a balance of CD4$^+$ T cell populations in the gut. Furthermore, our findings provide mechanistic insight into how the accumulation of immunosuppressive effector Treg populations is mediated following epithelial changes. Given the enormous clinical utility of strategies that target pathways inhibiting intratumoural immune responses, our data identifies a novel target which could potentially be manipulated to inhibit Treg accumulation in tumors with less of the deleterious side effects associated with current frontline therapeutics.

Acknowledgements:

Author contributions: H.M., A.B. and M.B. performed the experiments involving Cdh1$^{\Delta IEC}$ and KLRG1$^{-/-}$ mice, A.B. and A.I. performed the in vitro cultures, P.A. and M.Q-J. performed the APC$^{min/+}$ experiments, C.P. and S.B. performed the IL-33 staining on gut sections, A.B. and K.H. performed stable β-catenin mouse strain experiments. M.S. analyzed data and contributed essential reagents, A.I. directed research and wrote the paper with A.B. and input from all the authors.

We thank members of the Izcue lab for helpful discussions and comments on the manuscript, P. Rauf for help during initial work, K. Maloy for critical reading of the manuscript and R. Kemler for advice and material. Villin-Cre mice were generously provided by S. Robine. We are indebt to R. Hussong for outstanding technical help. We thank C. Johner, A. Ogboro, M. Pfunder, U. Stauffer, S. Burkart and the rest of the mouse facility staff for excellent animal care, and A. Wuerch, S. Hobitz and K. Schuldes for cell sorting.

This work was supported by the Bundesministerium für Bildung und Forschung (BMBF 01 EO 0803) and by the Max Planck Society. M. Q-J. and P.A. are supported by the Swedish Research Council and the Swedish Cancer Foundation. H.M. was supported by a Walter Hitzig fellowship of the Centre of Chronic Immunodeficiency, University Hospital Freiburg. A.B. is a member of the IMPRS-MCB, a joint international PhD programme of the Max Planck Institute of Immunobiology and Epigenetics and the University of Freiburg, Germany.

Conflict of interest: the authors signal no conflicting interest.

References:

1. Nishikawa H, Sakaguchi S. Regulatory T cells in cancer immunotherapy. Current opinion in immunology. 2014;27:1-7. Epub 2014/01/15.
2. Gallo RL, Hooper LV. Epithelial antimicrobial defence of the skin and intestine. Nature reviews Immunology. 2012;12(7):503-16. Epub 2012/06/26.
3. Peterson LW, Artis D. Intestinal epithelial cells: regulators of barrier function and immune homeostasis. Nature reviews Immunology. 2014;14(3):141-53. Epub 2014/02/26.
4. Wittkopf N, Neurath MF, Becker C. Immune-epithelial crosstalk at the intestinal surface. Journal of gastroenterology. 2014;49(3):375-87. Epub 2014/01/29.
5. Olszak T, Neves JF, Dowds CM, Baker K, Glickman J, Davidson NO, et al. Protective mucosal immunity mediated by epithelial CD1d and IL-10. Nature. 2014;509(7501):497-502. Epub 2014/04/11.
6. Josefowicz SZ, Lu LF, Rudensky AY. Regulatory T cells: mechanisms of differentiation and function. Annu Rev Immunol. 2012;30:531-64. Epub 2012/01/10.
7. Burzyn D, Benoist C, Mathis D. Regulatory T cells in nonlymphoid tissues. Nat Immunol. 2013;14(10):1007-13. Epub 2013/09/21.
8. Hegazy AN, Powrie F. MICROBIOME. Microbiota RORgulates intestinal suppressor T cells. Science. 2015;349(6251):929-30. Epub 2015/09/01.
9. Beyersdorf N, Ding X, Tietze JK, Hanke T. Characterization of mouse CD4 T cell subsets defined by expression of KLRG1. Eur J Immunol. 2007;37(12):3445-54. Epub 2007/11/24.
10. Feuerer M, Hill JA, Kretschmer K, von Boehmer H, Mathis D, Benoist C. Genomic definition of multiple ex vivo regulatory T cell subphenotypes. Proc Natl Acad Sci U S A. 2010;107(13):5919-24. Epub 2010/03/17.
11. Saito T, Nishikawa H, Wada H, Nagano Y, Sugiyama D, Atarashi K, et al. Two FOXP3(+)CD4(+) T cell subpopulations distinctly control the prognosis of colorectal cancers. Nature medicine. 2016;22(6):679-84. Epub 2016/04/26.
12. Plitas G, Konopacki C, Wu K, Bos PD, Morrow M, Putintseva EV, et al. Regulatory T Cells Exhibit Distinct Features in Human Breast Cancer. Immunity. 2016;45(5):1122-34. Epub 2016/11/17.
13. De Simone M, Arrigoni A, Rossetti G, Gruarin P, Ranzani V, Politano C, et al. Transcriptional Landscape of Human Tissue Lymphocytes Unveils Uniqueness of Tumor-Infiltrating T Regulatory Cells. Immunity. 2016;45(5):1135-47. Epub 2016/11/17.
14. Libusova L, Stemmler MP, Hierholzer A, Schwarz H, Kemler R. N-cadherin can structurally substitute for E-cadherin during intestinal development but leads to polyp formation. Development. 2010. Epub 2010/06/11.
15. Barker N, van Es JH, Kuipers J, Kujala P, van den Born M, Cozijnsen M, et al. Identification of stem cells in small intestine and colon by marker gene Lgr5. Nature. 2007;449(7165):1003-7. Epub 2007/10/16.
16. Harada N, Tamai Y, Ishikawa T, Sauer B, Takaku K, Oshima M, et al. Intestinal polyposis in mice with a dominant stable mutation of the beta-catenin gene. The EMBO journal. 1999;18(21):5931-42. Epub 1999/11/02.
17. Sanos SL, Diefenbach A. Isolation of NK cells and NK-like cells from the intestinal lamina propria. Methods Mol Biol. 2010;612:505-17. Epub 2009/12/25.

18. Izcue A, Hue S, Buonocore S, Arancibia-Carcamo CV, Ahern PP, Iwakura Y, et al. Interleukin-23 restrains regulatory T cell activity to drive T cell-dependent colitis. Immunity. 2008;28(4):559-70. Epub 2008/04/11.
19. Wirtz S, Neufert C, Weigmann B, Neurath MF. Chemically induced mouse models of intestinal inflammation. Nat Protoc. 2007;2(3):541-6. Epub 2007/04/05.
20. Maywald RL, Doerner SK, Pastorelli L, De Salvo C, Benton SM, Dawson EP, et al. IL-33 activates tumor stroma to promote intestinal polyposis. Proc Natl Acad Sci U S A. 2015;112(19):E2487-96. Epub 2015/04/29.
21. Lupar E, Brack M, Garnier L, Laffont S, Rauch KS, Schachtrup K, et al. Eomesodermin Expression in CD4+ T Cells Restricts Peripheral Foxp3 Induction. J Immunol. 2015;195(10):4742-52. Epub 2015/10/11.
22. Reich M, Liefeld T, Gould J, Lerner J, Tamayo P, Mesirov JP. GenePattern 2.0. Nature genetics. 2006;38(5):500-1. Epub 2006/04/28.
23. Gene Ontology Consortium. Gene Ontology Consortium: going forward. Nucleic acids research. 2015;43(Database issue):D1049-56. Epub 2014/11/28.
24. Cheng G, Yuan X, Tsai MS, Podack ER, Yu A, Malek TR. IL-2 receptor signaling is essential for the development of Klrg1+ terminally differentiated T regulatory cells. J Immunol. 2012;189(4):1780-91. Epub 2012/07/13.
25. Tauro S, Nguyen P, Li B, Geiger TL. Diversification and senescence of Foxp3+ regulatory T cells during experimental autoimmune encephalomyelitis. Eur J Immunol. 2013;43(5):1195-207. Epub 2013/02/26.
26. Miyara M, Yoshioka Y, Kitoh A, Shima T, Wing K, Niwa A, et al. Functional delineation and differentiation dynamics of human CD4+ T cells expressing the FoxP3 transcription factor. Immunity. 2009;30(6):899-911. Epub 2009/05/26.
27. Huehn J, Siegmund K, Lehmann JC, Siewert C, Haubold U, Feuerer M, et al. Developmental stage, phenotype, and migration distinguish naive- and effector/memory-like CD4+ regulatory T cells. J Exp Med. 2004;199(3):303-13. Epub 2004/02/06.
28. Blatner NR, Bonertz A, Beckhove P, Cheon EC, Krantz SB, Strouch M, et al. In colorectal cancer mast cells contribute to systemic regulatory T-cell dysfunction. Proc Natl Acad Sci U S A. 2010;107(14):6430-5. Epub 2010/03/24.
29. Wohlfert EA, Grainger JR, Bouladoux N, Konkel JE, Oldenhove G, Ribeiro CH, et al. GATA3 controls Foxp3+ regulatory T cell fate during inflammation in mice. J Clin Invest. 2011. Epub 2011/10/04.
30. Wang Y, Su MA, Wan YY. An essential role of the transcription factor GATA-3 for the function of regulatory T cells. Immunity. 2011;35(3):337-48. Epub 2011/09/20.
31. Rudra D, deRoos P, Chaudhry A, Niec RE, Arvey A, Samstein RM, et al. Transcription factor Foxp3 and its protein partners form a complex regulatory network. Nat Immunol. 2012;13(10):1010-9. Epub 2012/08/28.
32. Sawant DV, Sehra S, Nguyen ET, Jadhav R, Englert K, Shinnakasu R, et al. Bcl6 controls the Th2 inflammatory activity of regulatory T cells by repressing Gata3 function. J Immunol. 2012;189(10):4759-69.
33. Farin HF, Van Es JH, Clevers H. Redundant sources of Wnt regulate intestinal stem cells and promote formation of Paneth cells. Gastroenterology. 2012;143(6):1518-29 e7.
34. Clevers H, Nusse R. Wnt/beta-catenin signaling and disease. Cell. 2012;149(6):1192-205. Epub 2012/06/12.

35. Fridman WH, Pages F, Sautes-Fridman C, Galon J. The immune contexture in human tumours: impact on clinical outcome. Nature reviews Cancer. 2012;12(4):298-306.
36. Su LK, Kinzler KW, Vogelstein B, Preisinger AC, Moser AR, Luongo C, et al. Multiple intestinal neoplasia caused by a mutation in the murine homolog of the APC gene. Science. 1992;256(5057):668-70.
37. Brannon AR, Vakiani E, Sylvester BE, Scott SN, McDermott G, Shah RH, et al. Comparative sequencing analysis reveals high genomic concordance between matched primary and metastatic colorectal cancer lesions. Genome biology. 2014;15(8):454. Epub 2014/08/29.
38. Zeineldin M, Neufeld KL. Understanding phenotypic variation in rodent models with germline Apc mutations. Cancer research. 2013;73(8):2389-99.
39. Akeus P, Langenes V, Kristensen J, von Mentzer A, Sparwasser T, Raghavan S, et al. Treg-cell depletion promotes chemokine production and accumulation of CXCR3(+) conventional T cells in intestinal tumors. Eur J Immunol. 2015;45(6):1654-66. Epub 2015/03/11.
40. Schiering C, Krausgruber T, Chomka A, Frohlich A, Adelmann K, Wohlfert EA, et al. The alarmin IL-33 promotes regulatory T-cell function in the intestine. Nature. 2014. Epub 2014/07/22.
41. Nakanishi Y, Seno H, Fukuoka A, Ueo T, Yamaga Y, Maruno T, et al. Dclk1 distinguishes between tumor and normal stem cells in the intestine. Nature genetics. 2013;45(1):98-103. Epub 2012/12/04.
42. Burzyn D, Kuswanto W, Kolodin D, Shadrach JL, Cerletti M, Jang Y, et al. A special population of regulatory T cells potentiates muscle repair. Cell. 2013;155(6):1282-95. Epub 2013/12/10.
43. Arpaia N, Green JA, Moltedo B, Arvey A, Hemmers S, Yuan S, et al. A Distinct Function of Regulatory T Cells in Tissue Protection. Cell. 2015;162(5):1078-89. Epub 2015/09/01.
44. Arteaga CL, Engelman JA. ERBB receptors: from oncogene discovery to basic science to mechanism-based cancer therapeutics. Cancer cell. 2014;25(3):282-303. Epub 2014/03/22.
45. Worthington JJ, Kelly A, Smedley C, Bauche D, Campbell S, Marie JC, et al. Integrin alphavbeta8-Mediated TGF-beta Activation by Effector Regulatory T Cells Is Essential for Suppression of T-Cell-Mediated Inflammation. Immunity. 2015;42(5):903-15. Epub 2015/05/17.
46. Manetti M, Ibba-Manneschi L, Liakouli V, Guiducci S, Milia AF, Benelli G, et al. The IL1-like cytokine IL33 and its receptor ST2 are abnormally expressed in the affected skin and visceral organs of patients with systemic sclerosis. Annals of the rheumatic diseases. 2010;69(3):598-605. Epub 2009/09/26.

Figure Legends

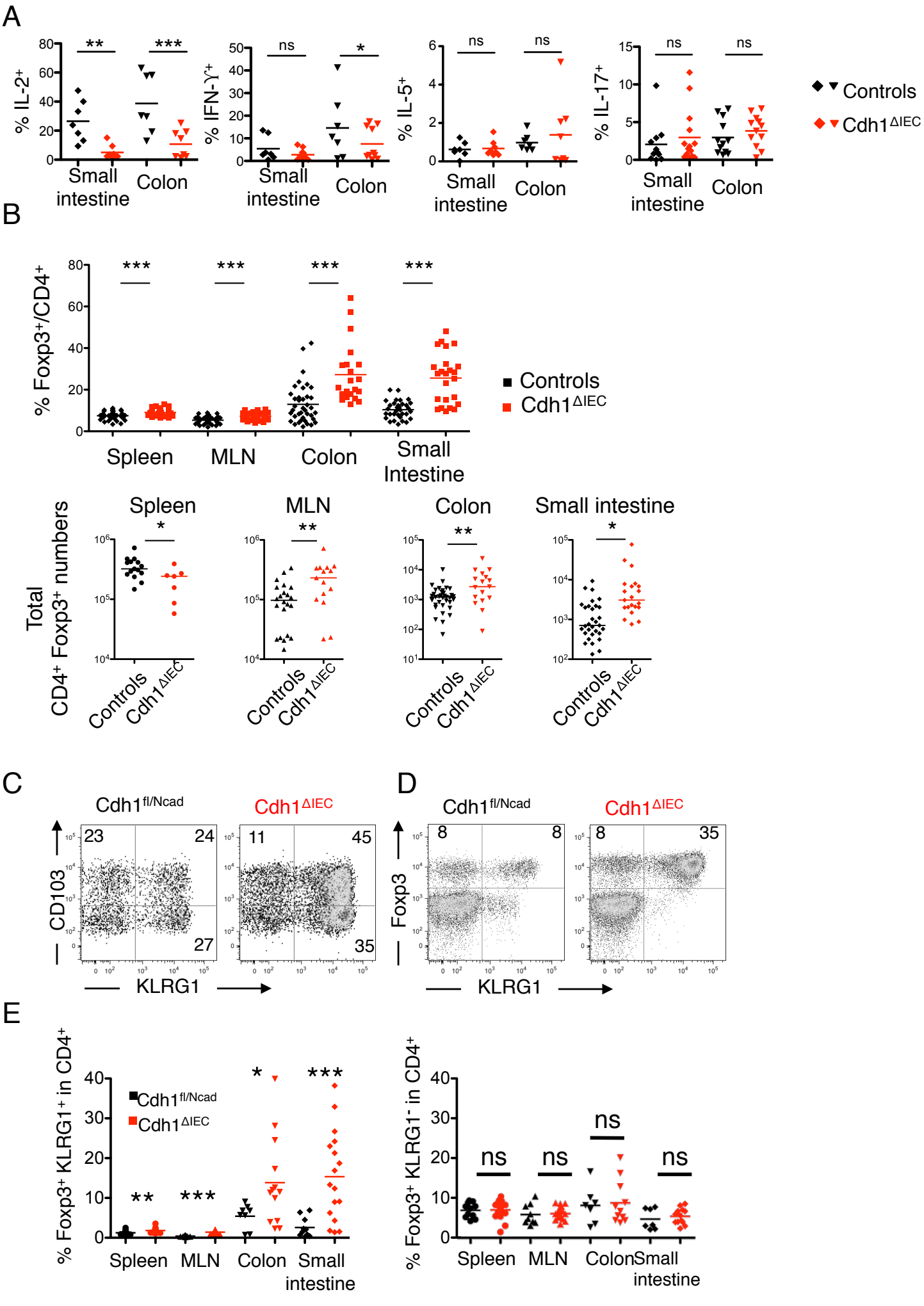
A
% IL-2+
% IFN-γ+
% IL-5+
% IL-17+
Small intestine
Colon
Controls
Cdh1ΔIEC
B
% Foxp3+/CD4+
Spleen
MLN
Colon
Small Intestine
Total CD4+ Foxp3+ numbers
C
Cdh1fl/Ncad
Cdh1ΔIEC
CD103
KLRG1
D
Foxp3
E
% Foxp3+ KLRG1+ in CD4+
% Foxp3+ KLRG1- in CD4+
ns

Figure 1

FIGURE 1: Treg expressing the E-cadherin receptor KLRG1 accumulate in the gut of Cdh1$^{\Delta IEC}$ mice (A) Cytokine production by CD4^{+} Foxp3^{-} T cells from the small intestine or colon of Cdh1$^{\Delta IEC}$ mice or control littermates. Data are pooled from 2 (IL-2) or 3 (IFN-γ, IL-5, IL-17A) independent experiments. **(B)** Top row, Foxp3^{+} frequencies among CD4^{+} T cells in Cdh1$^{\Delta IEC}$ mice or control littermates. Bottom row, absolute numbers of Foxp3^{+} CD4^{+} cells in Cdh1$^{\Delta IEC}$ mice and control littermates. **(C)** Representative plots of KLRG1 versus CD103 expression among CD4^{+} Foxp3^{+} T cells from the colonic lamina propria of Cdh1$^{\Delta IEC}$ mice and control littermates. **(D)** Representative plots of KLRG1 versus Foxp3 expression among CD4^{+} T cells from colonic lamina propria of Cdh1$^{\Delta IEC}$ mice and control littermates. **(E)** Frequencies of Foxp3^{+} KLRG1^{+} (left) or Foxp3^{+} KLRG1^{-} (right) among CD4^{+} T cells in the indicated organs in Cdh1$^{\Delta IEC}$ mice or control littermates. Black symbols, Cdh1$^{fl/Ncad}$ controls; red symbols, Cdh1$^{\Delta IEC}$ mice. All mice were analyzed at the age of 3 weeks, because the lethality observed in Cdh1$^{\Delta IEC}$ mice precluded analysis at later time points. Mice of both sexes were used for the analyses. Each point corresponds to an individual mouse. *p<0.05; **p<0.01; ***p<0.001; ns, not significant compared to Cdh1$^{fl/Ncad}$ controls.

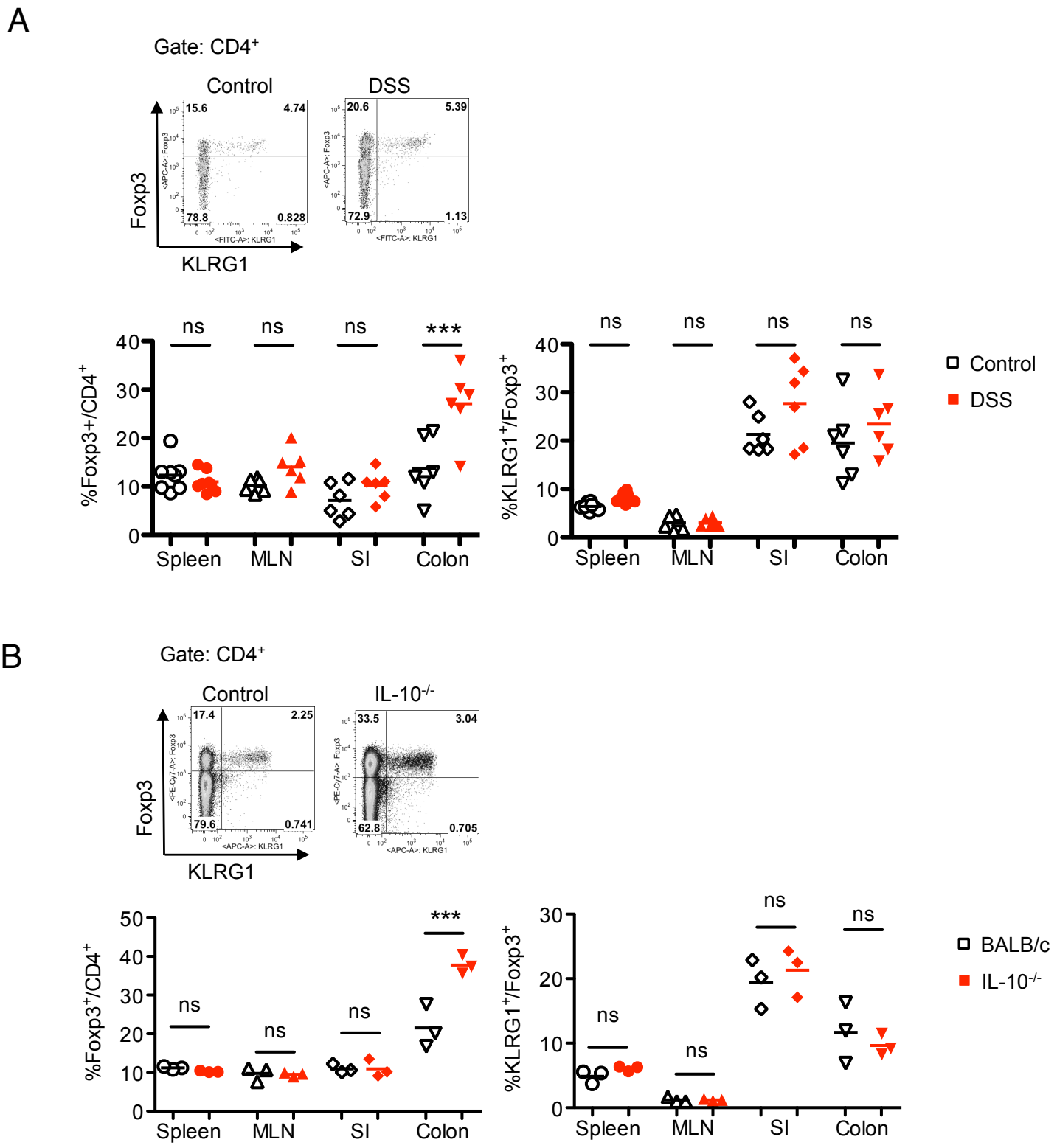
A
Gate: CD4+
Control
DSS
15.6
4.74
78.8
0.828
20.6
5.39
72.9
1.13
Foxp3
KLRG1
%Foxp3+/CD4+
%KLRG1+/Foxp3+
ns
***
Spleen
MLN
SI
Colon
Control
DSS
B
Gate: CD4+
Control
IL-10-/-
17.4
2.25
79.6
0.741
33.5
3.04
62.8
0.705
%Foxp3+/CD4+
%KLRG1+/Foxp3+
BALB/c
IL-10-/-

Figure 2

FIGURE 2: Inflammation does not drive specific KLRG1$^+$ Treg accumulation.

(A) Treg populations in DSS-treated mice. 8 - 9 week old mice were treated for 8 days with 3%DSS or water, and analysed immediately after the treatment stopped. Top: the plot shows representative KLRG1 and Foxp3 expression among TCRβ$^+$ CD4$^+$ T cells from the colonic lamina propria and untreated control mice. Bottom left, frequencies of Foxp3$^+$ cells among CD4$^+$ in the indicated organs. Bottom right, frequencies of KLRG1$^+$ cells among CD4$^+$ Foxp3$^+$ cells in the indicated organs. Data are pooled from 2 independent experiments with three mice per group/experiment. Both females and males were used. (B) Treg populations in IL-10-deficient mice and control littermates. Data show one representative experiment out of two; plots as in (A). Each point corresponds to an individual mouse; 8-week old IL-10-deficient mice (two females, one male) and sex-matched heterozygous littermates were used. *$p<0.05$; **$p<0.01$; ns, not significant compared to controls.

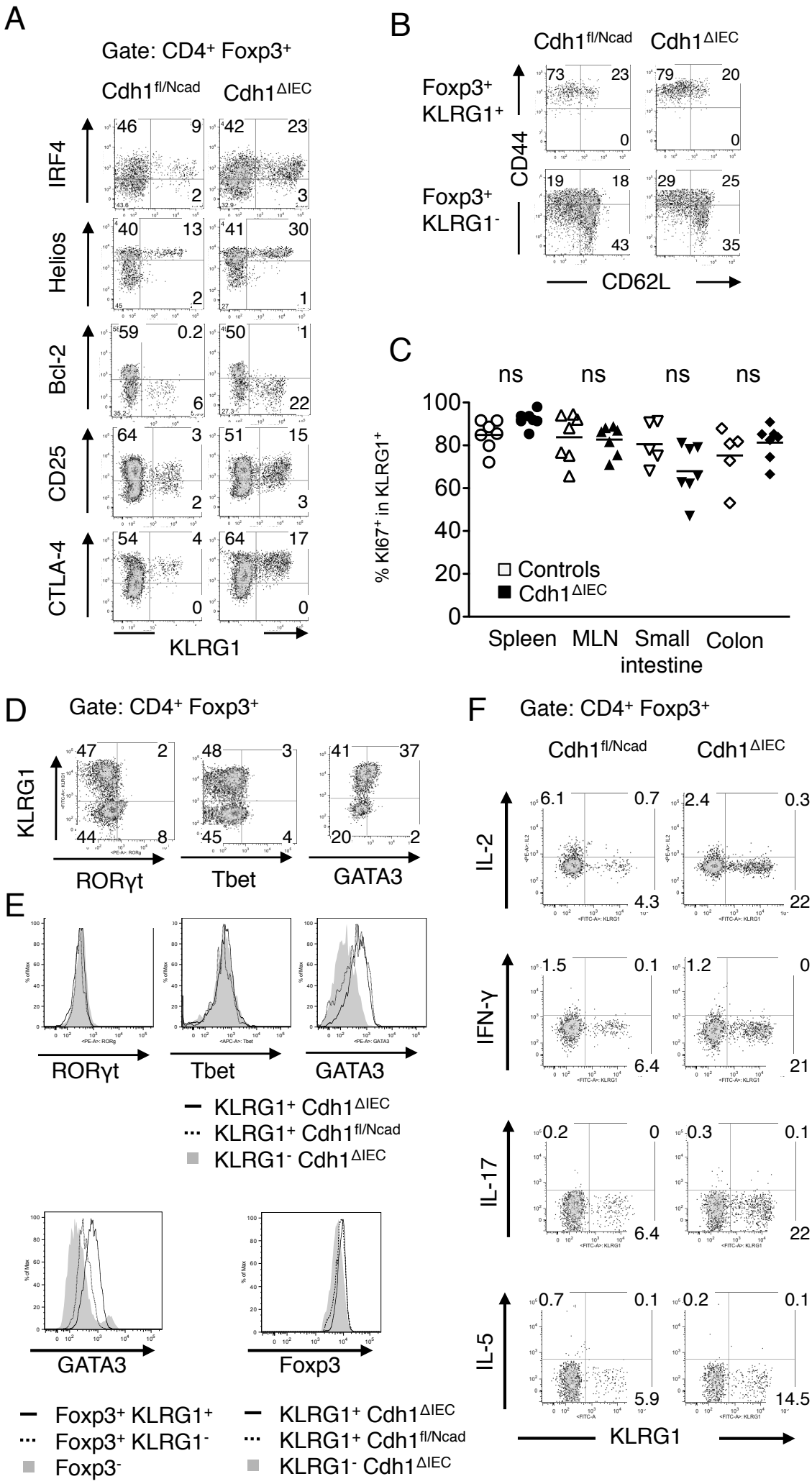
A
Gate: CD4+ Foxp3+
Cdh1fl/Ncad
Cdh1ΔIEC
IRF4
Helios
Bcl-2
CD25
CTLA-4
KLRG1
B
Cdh1fl/Ncad
Cdh1ΔIEC
Foxp3+ KLRG1+
Foxp3+ KLRG1-
CD44
CD62L
C
ns
% KI67+ in KLRG1+
Controls
Cdh1ΔIEC
Spleen
MLN
Small intestine
Colon
D
Gate: CD4+ Foxp3+
KLRG1
RORγt
Tbet
GATA3
E
RORγt
Tbet
GATA3
KLRG1+ Cdh1ΔIEC
KLRG1+ Cdh1fl/Ncad
KLRG1- Cdh1ΔIEC
GATA3
Foxp3
Foxp3+ KLRG1+
Foxp3+ KLRG1-
Foxp3-
KLRG1+ Cdh1ΔIEC
KLRG1+ Cdh1fl/Ncad
KLRG1- Cdh1ΔIEC
F
Gate: CD4+ Foxp3+
Cdh1fl/Ncad
Cdh1ΔIEC
IL-2
IFN-γ
IL-17
IL-5
KLRG1

Figure 3

FIGURE 3: KLRG1$^+$ Treg have an E-cadherin-independent activated phenotype and belong to the GATA3$^+$ Treg subset

(**A**) KLRG1 versus indicated activation markers in CD4$^+$ Foxp3$^+$ lymphocytes from the MLN of control Cdh1$^{fl/Ncad\ KI}$ (left) and littermate Cdh1$^{\Delta IEC}$ mice. (**B**) CD44 and CD62L expression among Foxp3$^+$ KLRG1$^+$ (top) and Foxp3$^+$ KLRG1$^-$ (bottom) CD4$^+$ T cells from the MLN of control Cdh1$^{fl/Ncad\ KI}$ (left) and littermate Cdh1$^{\Delta IEC}$mice. (**C**) Frequency of proliferating Ki67$^+$ cells among MLN KLRG1$^+$ CD4$^+$ Foxp3$^+$ T cells. Each symbol shows data from a single mouse, data are pooled from 3 independent experiments. (**D**) Expression of RORγt, Tbet and GATA3 in CD4$^+$ Foxp3$^+$ cells isolated from the colonic lamina propria of Cdh1$^{\Delta IEC}$ mice. Plots are representative of three independent analyses. (**E**) Expression of lineage-defining transcription factors in Foxp3$^+$ KLRG1$^+$ CD4$^+$ T cells from the colonic lamina propria. Top: cells from Cdh1$^{\Delta IEC}$ (continuous line) and littermate Cdh1$^{fl/Ncad}$ (dotted line) compared to CD4$^+$ Foxp3$^+$ KLRG1$^-$ T cells from the same Cdh1$^{\Delta IEC}$ mouse (grey solid histogram). Bottom left: GATA3 expression in KLRG1$^+$ (dotted line) and KLRG1$^-$ (continuous line) Foxp3$^+$ CD4$^+$ T cells compared to Foxp3$^-$ CD4$^+$ T cells (grey solid histogram). Bottom right: Foxp3 expression in T cell subsets as in top. (**F)** IL-2, IFN-γ, IL-5 and IL-17A secretion by CD4$^+$ Foxp3$^+$ cells from the MLN of control Cdh1$^{fl/Ncad\ KI}$ (left) and littermate Cdh1$^{\Delta IEC}$ (right) mice. All data shown are representative of two or three independent experiments with at least one 3-week-old Cdh1$^{\Delta IEC}$ and one littermate control Cdh1$^{fl/Ncad\ KI}$ mice. Mice of both sexes were used for the analyses.

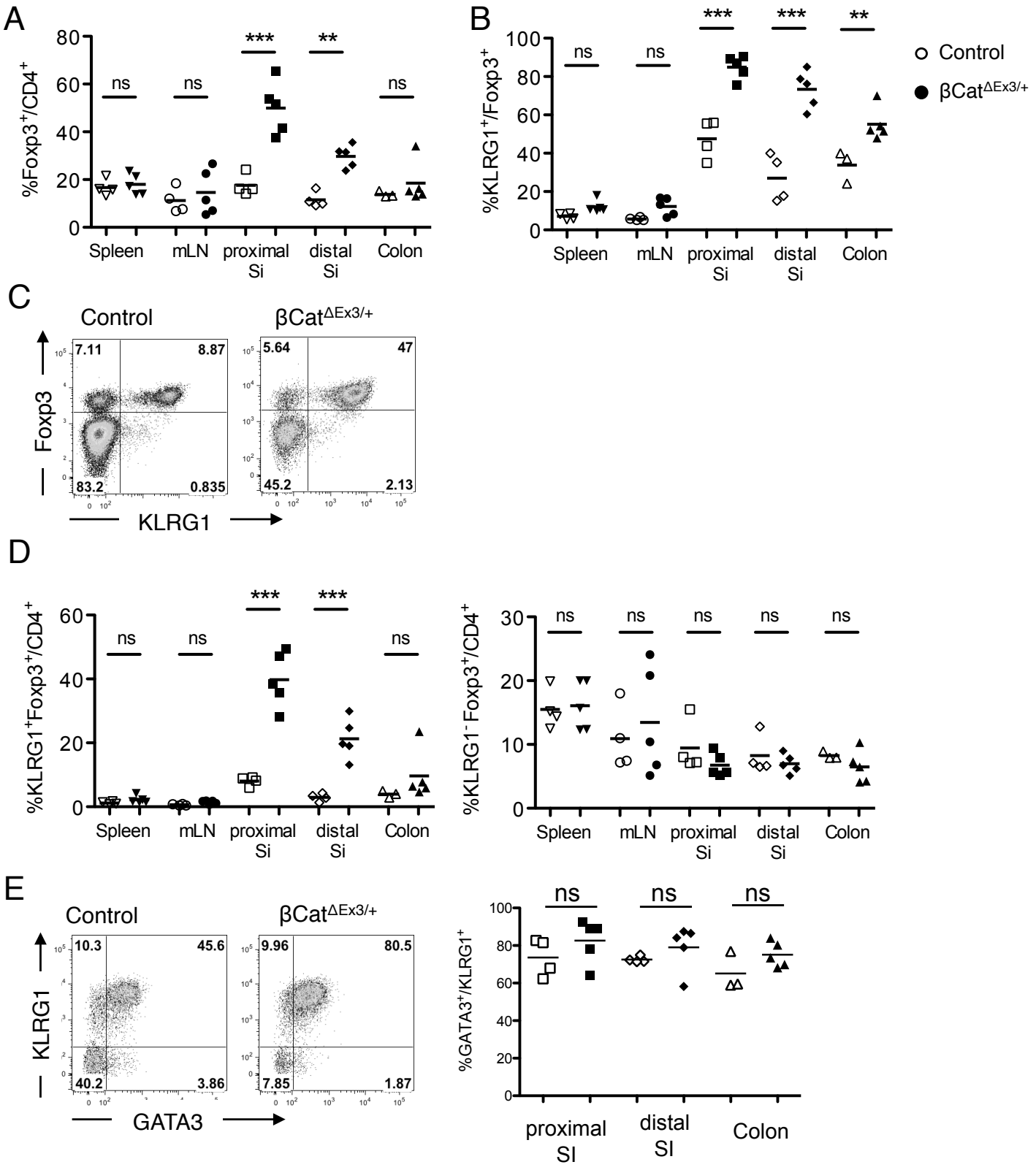
A
%Foxp3+/CD4+
ns
ns
***
**
ns
Spleen
mLN
proximal Si
distal Si
Colon
B
%KLRG1+/Foxp3+
ns
ns
***
***
**
Control
βCatΔEx3/+
C
Control
βCatΔEx3/+
Foxp3
KLRG1
7.11
8.87
83.2
0.835
5.64
47
45.2
2.13
D
%KLRG1+Foxp3+/CD4+
%KLRG1-Foxp3+/CD4+
E
Control
βCatΔEx3/+
KLRG1
GATA3
10.3
45.6
40.2
3.86
9.96
80.5
7.85
1.87
%GATA3+/KLRG1+
proximal SI
distal SI
Colon

Figure 4

FIGURE 4: Epithelial β-catenin expands the intestinal Treg compartment through the accumulation of KLRG1$^+$ Treg. (A) Frequency of Foxp3$^+$ among CD4$^+$ T cells from tamoxifen-treated mice with the active β-catenin construct (filled; Ctnnb1$^{(Ex3)fl/+}$ Lgr5-EGFP-IRES-ERT2:Cre$^+$, called here βCat$^{\Delta Ex3/+}$) and control mice (empty; Ctnnb1$^{+/+}$ Lgr5-EGFP-IRES-ERT2:Cre$^+$ or Ctnnb1$^{(Ex3)fl/+}$). **(B)** Frequency of KLRG1$^+$ cells among Foxp3$^+$ CD4$^+$ T cells from mice as in (A). **(C)** Representative plots of KLRG1 and Foxp3 expression in CD4$^+$ T cells from the proximal small intestinal lamina propria. **(D)** Frequency of Foxp3$^+$ KLRG1$^+$ (left) or Foxp3$^+$ KLRG1$^-$ (right) among CD4$^+$ T cells from mice as in (A). **(E)** Representative plot of GATA3 expression in proximal small intestinal lamina propria Foxp3$^+$ CD4$^+$ T cells from mice as in (A), and frequencies of GATA3$^+$ cells among intestinal KLRG1$^+$ Foxp3$^+$ cells. Data shown are from two independent experiments. 8 to 9 months old mice of both sexes were used. Each point represents an individual mouse, with a total of 4 control and 5 βCat$^{\Delta Ex3/+}$ mice. ***p<0.001; **p<0.01; *p<0.05; ns, not significant.

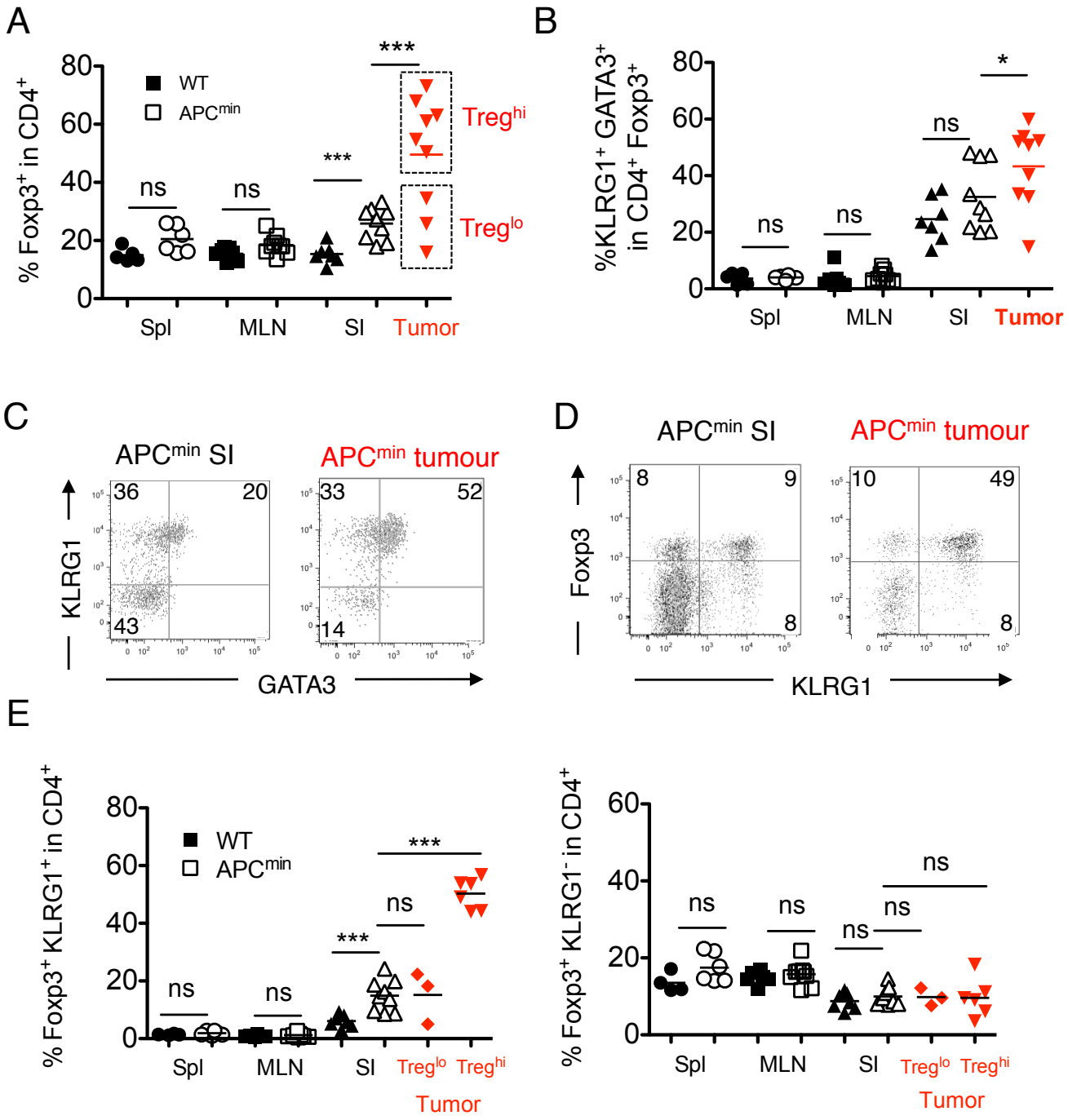
A
% Foxp3+ in CD4+
WT
APCmin
Treghi
Treglo
ns
***
Spl
MLN
SI
Tumor
B
%KLRG1+ GATA3+ in CD4+ Foxp3+
*
C
APCmin SI
APCmin tumour
KLRG1
GATA3
36
20
43
33
52
14
D
Foxp3
KLRG1
8
9
10
49
E
% Foxp3+ KLRG1+ in CD4+
% Foxp3+ KLRG1- in CD4+

Figure 5

FIGURE 5: Intestinal tumors promote the accumulation of KLRG1$^+$ Treg. (A) Frequency of Foxp3$^+$ cells among CD4$^+$ T cells from APC$^{min/+}$ (filled black symbols), intestinal tumors of APC$^{min/+}$ (filled red symbols) and control mice (empty symbols). Dashed boxed indicate tumors with (Treg^{hi}) or without (Treg^{lo}) accumulation of Foxp3$^+$ T cells. **(B)** Frequencies of KLRG1$^+$ GATA3$^+$ cells among CD4$^+$ Foxp3$^+$ and **(C)** representative plot of KLRG1 and GATA3 expression in Foxp3$^+$ CD4$^+$ T cells from the indicated organs of mice as in (A). **(D)** Representative plots of KLRG1 and Foxp3 expression in CD4$^+$ T cells from the indicated organ and **(E)** frequency of Foxp3$^+$ KLRG1$^+$ (left) or Foxp3$^+$ KLRG1$^-$ (right) among CD4$^+$ T cells from mice as in (A). Data shown are from three independent experiments. Each point represents an individual mouse, a total of 7 control and 9 APC$^{min/+}$ mice were used. Mice were 18-21 weeks old when analyzed. Mice from both sexes were used for this study. Small intestinal tumors with a diameter between 1-4 mm were analyzed ***$p<0.001$; **$p<0.01$; *$p<0.05$; ns, not significant.

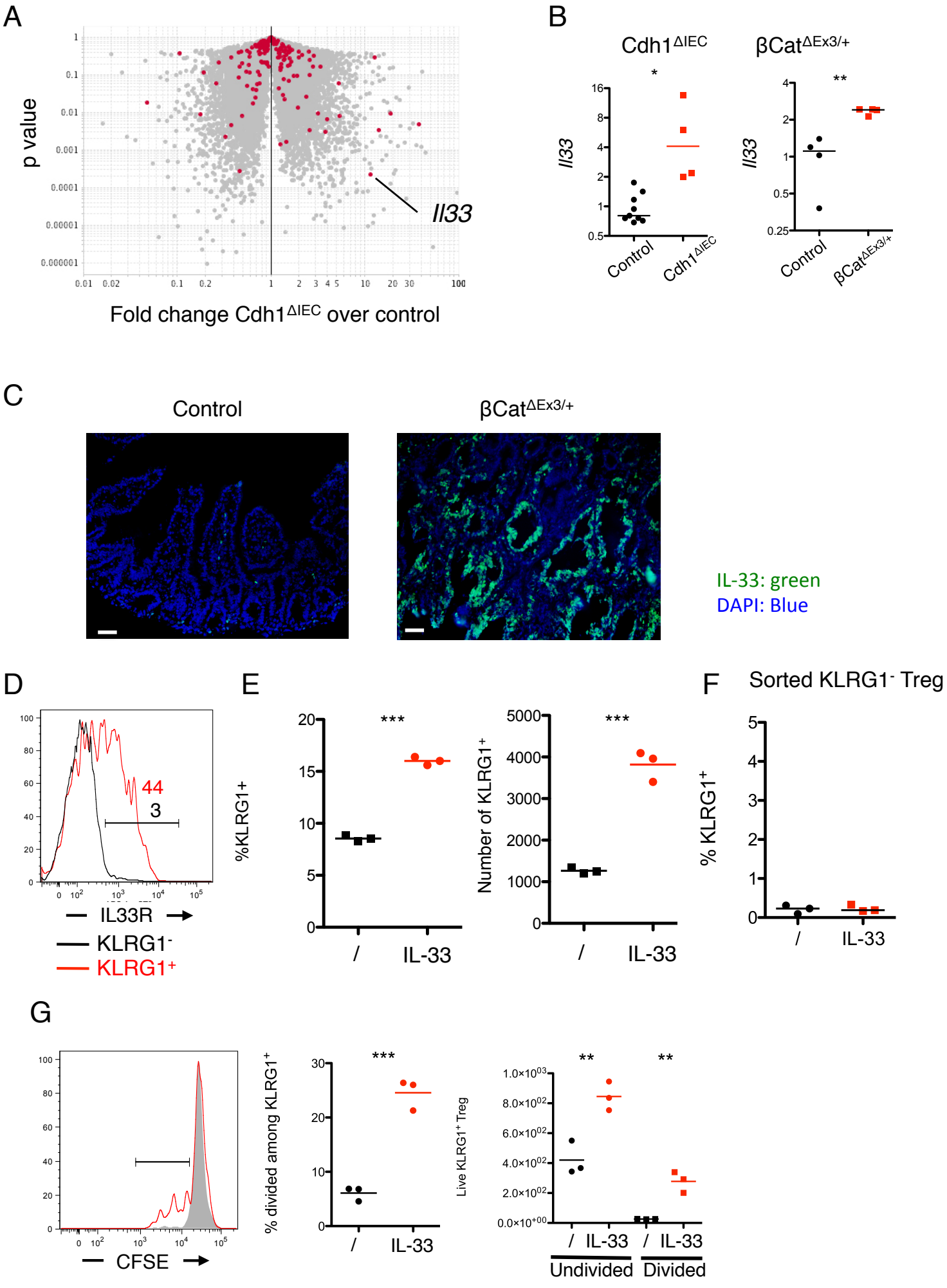
A
p value
Il33
Fold change Cdh1ΔIEC over control
B
Cdh1ΔIEC
βCatΔEx3/+
Il33
Control
Cdh1ΔIEC
βCatΔEx3/+
C
Control
βCatΔEx3/+
IL-33: green
DAPI: Blue
D
44
3
IL33R
KLRG1-
KLRG1+
E
%KLRG1+
Number of KLRG1+
/
IL-33
F
Sorted KLRG1- Treg
% KLRG1+
G
CFSE
% divided among KLRG1+
Live KLRG1+ Treg
Undivided
Divided

Figure 6

FIGURE 6: Increased β-catenin signals induce IL-33 in intestinal epithelial cells.

(A) Volcano plot showing fold change versus statistical significance of genes expressed in intestinal epithelial cells from 2-week old $Cdh1^{\Delta IEC}$ mice compared to control littermates, as analyzed by microarray (GSE81920; http://www.ncbi.nlm.nih.gov/geo/query/acc.cgi?token=whmzwqekprydpsz&acc=GSE81920). Each dot represents one transcript. Genes highlighted in red are those with cytokine activity (Gene Ontology term GO:0005125, *Mus musculus*) **(B)** *Il33* expression in intestinal epithelial cells from $Cdh1^{\Delta IEC}$ mice (3 week-old) and control littermates or $\beta Cat^{\Delta Ex3/+}$ and control mice, as measured by qPCR. $\beta Cat^{\Delta Ex3/+}$ and control samples were taken from mice analyzed in Figure 4. Each dot represents one mouse. Values are normalized to *Hprt* expression in each sample. (C) IL-33 expression in small intestine from control (left) or $\beta Cat^{\Delta Ex3/+}$ (right) mice. Tissue was taken from the mice analyzed in Figure 4. Bar represents 50 µm. **(D)** Expression of IL-33 receptor on activated $KLRG1^+$ (red line and number) and $KLRG1^-$ (black line and number) Treg. Sorted C57BL/6 $CD25^+$ T cells were stimulated for 3 days with plate-bound anti-CD3 and stained for Foxp3, KLRG1 and IL-33 receptor. Histograms are gated on Viability Dye^- $CD4^+$ $Foxp3^+$ $KLRG1^+$ or $KLRG1^-$ cells. Numbers show the frequency of IL-33 receptor-positive cells. Data are representative of two independent experiments. **(E)** Frequency (left) and total numbers (right) of $KLRG1^+$ cells among $CD4^+$ $Foxp3^+$ live cells 3 days after culture of sorted C57BL/6 Treg with anti-CD3 with or without 5 ng/ml of IL-33. **(F)** Frequency of $KLRG1^+$ cells after sorted C57BL/6 $KLRG1^-$ Treg were cultured as in (E). Cultures are representative of 2 to 4 independent experiments each. ***$p<0.001$; **$p<0.01$; *$p<0.05$. **(G)** Sorted $KLRG1^+$ Treg were labeled with CFSE and mixed 1:10 with $KLRG1^-$ Treg. Cells were cultured as in (E). Left,

representative plot of CFSE signal in cells cultured with (red line) or without (grey histogram) IL-33. Bar shows divided cells. Center, frequency of divided cells among live KLRG1^{+}. Right, total numbers of divided and undivided live cells. Data are representative of two independent experiments.

Supplementary Figures

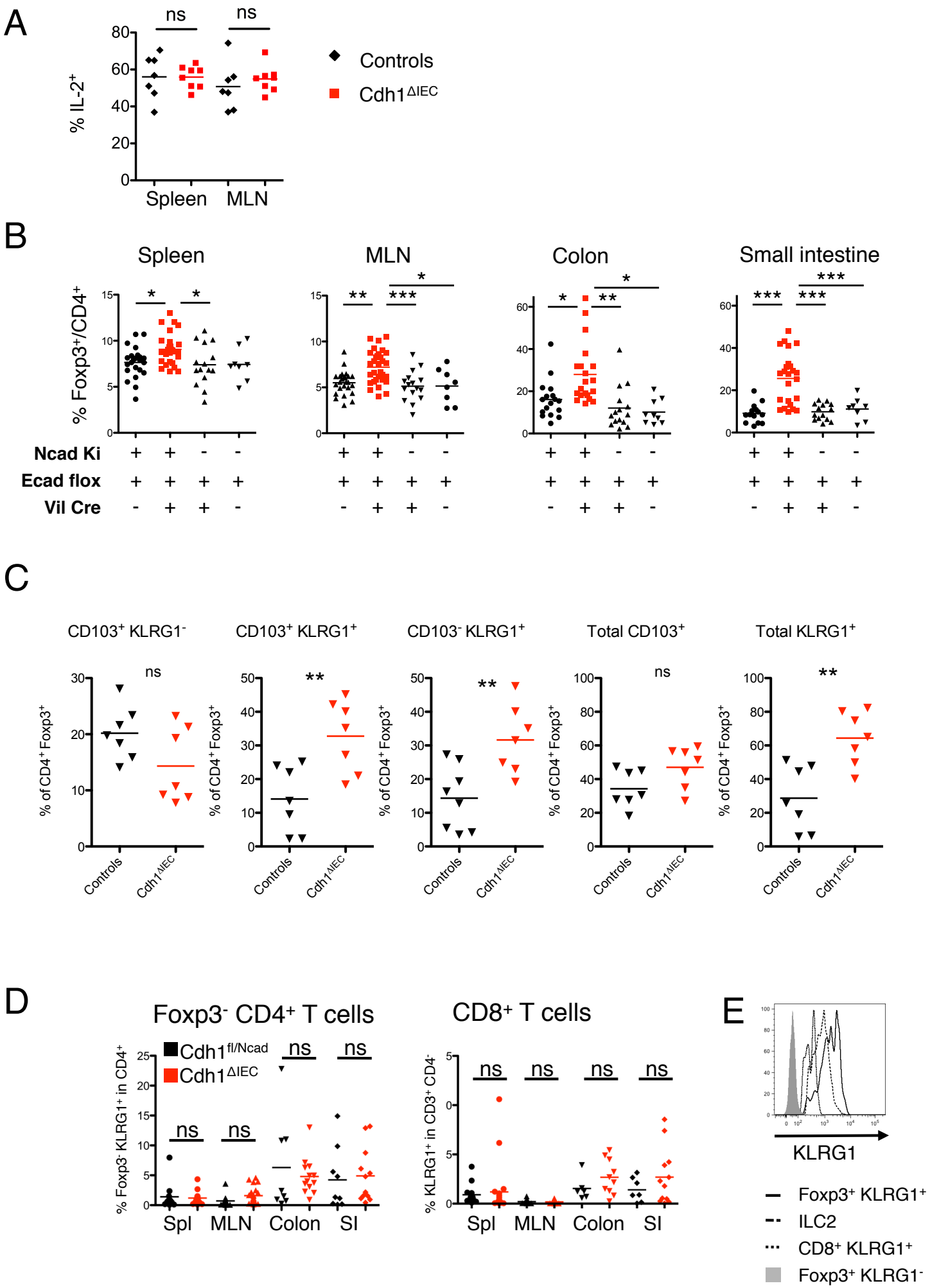

Supplementary Figure 1

FIGURE S1. (A) IL-2 production by $CD4^+$ $Foxp3^-$ T cells from the spleen or MLN of $Cdh1^{\Delta IEC}$ mice or control littermates. Data are pooled from 2 independent experiments. **(B)** Frequencies of $Foxp3^+$ among $CD4^+$ T cells from mice of the indicated genotypes. **(C)** Frequencies of $CD103^+$ $KLRG1^-$, $CD103^+$ $KLRG1^+$ and $CD103^-$ $KLRG1^+$ cells, total $CD103^+$ cells and total $KLRG1^+$ cells among colonic $CD4^+$ $Foxp3^+$ T cells from 3-week-old SPF $Cdh1^{\Delta IEC}$ mice (red) and control littermates (black). Both $CD103^+$ and $CD103^-$ $KLRG1^+$ Treg are increased in $Cdh1^{\Delta IEC}$ mice, while $CD103^+$ $KLRG1^-$ Treg are not increased. **(D)** Frequencies of $Foxp3^-$ $KLRG1^+$ among $CD4^+$ T cells (left) and $KLRG1^+$ among $CD3^+$ $CD4^-$ T cells (mostly $CD8^+$ T cells) (right) from 3-week-old SPF $Cdh1^{\Delta IEC}$ mice (red) and $Cdh1^{fl/Ncad}$ control littermates (black). Each point corresponds to an individual mouse. Data are pooled from at least 3 independent analyses. *$p<0.05$; **$p<0.01$; ***$p<0.001$; ns, not significant. **(E)** Comparison of KLRG1 levels on different $KLRG1^+$ small intestinal lymphoid populations. Solid line: $CD4^+$ $Foxp3^+$ $KLRG1^+$ cells, dotted line: $CD8^+$ $KLRG1^+$ cells, dashed line: $TCR\beta^-$ $GATA3^{hi}$ $KLRG1^+$ ILC2 cells. Grey histogram, control $CD4^+$ $Foxp3^+$ $KLRG1^-$ cells. The frequency of $CD4^+$ $Foxp3^-$ $KLRG1^+$ cells is very low; KLRG1 levels can be seen in Figure 1D.

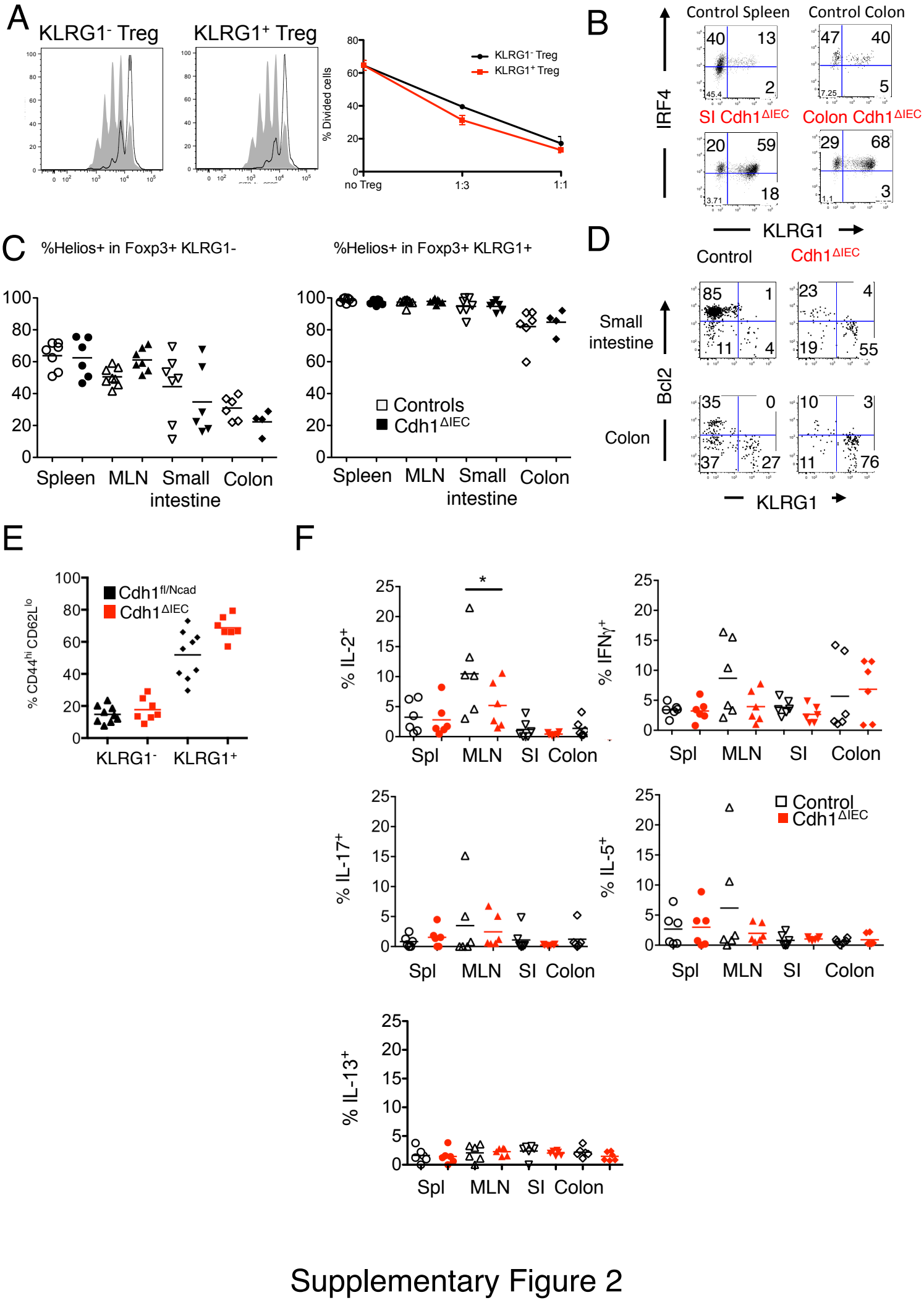

Supplementary Figure 2

FIGURE S2: Characteristics of KLRG1$^+$ Treg (A) KLRG1$^+$ Treg are suppressive in vitro. CFSE-labeled CD25$^-$ CD4$^+$ T cells were cultured with sorted KLRG1$^-$ or KLRG1$^+$ CD25$^+$ T cells at different ratios. The histograms show CFSE signal after 3 days of culture without Treg (grey) or with 1:1 KLRG1$^-$ (left plot, black line) or KLRG1$^+$ (central plot, black line) CD25$^+$ T cells. Plots are gated on CFSE$^+$ cells. Right, frequency of divided CFSE$^+$ cells after 3 days of culture with different numbers of KLRG1$^+$ (red) or KLRG1$^-$ (black) CD25$^+$ T cells. Data show mean +/- SD of three replicates and they are representative of two independent experiments. **(B)** Dot plot showing KLRG1 versus IRF4 expression in CD4$^+$ Foxp3$^+$ KLRG1$^+$ Treg from colon and small intestine from a Cdh1$^{\Delta IEC}$ mouse; IRF4 showing spleen (non-tissue organ harbouring IRF4$^-$ cells) and colon from a control littermate are shown on top as a reference. **(C)** Frequencies of Helios-expressing cells among Foxp3$^+$ KLRG1$^-$ (left) and Foxp3$^+$ KLRG1$^+$ (right) cells from control (empty) and littermate SPF Cdh1$^{\Delta IEC}$ mice (filled symbols). Data shown are pooled from three independent experiments. Each dot represents an individual mouse. **(D)** Dot plot showing KLRG1 versus Bcl-2 expression in CD4$^+$ Foxp3$^+$ KLRG1$^+$ Treg from colon and small intestine from a Cdh1$^{\Delta IEC}$ mouse and control littermate. **(E)** Frequency of CD44^{hi} CD62L^{lo} among Foxp3$^+$ KLRG1$^-$ (left) and Foxp3$^+$ KLRG1$^+$ (right) from MLN of control (black) and littermate SPF Cdh1$^{\Delta IEC}$ mice (red symbols). Data shown are pooled from three independent experiments. Each dot represents an individual mouse. **(F)** IL-2, IFN-γ, IL-17, IL-5 and IL-13 secretion by CD4$^+$ Foxp3$^+$ KLRG1$^+$ cells from the indicated organs of control (empty) and littermate SPF Cdh1$^{\Delta IEC}$ mice (red symbols). Data shown are pooled from two independent experiments. Each dot represents an individual mouse.